*Bioelectromagnetics*

RESEARCH ARTICLE OPEN ACCESS

# Dual Evaluation and Spatial Analysis of RF-EMF Exposure in 5G: Theoretical Extrapolations and Direct Measurements

Alberto Najera[1,2] | Alvaro Villaescusa-Tebar[3] | Jesus Gonzalez-Rubio[1,2] | Concepcion Garcia-Pardo[3]

[1]Department of Medical Sciences. Faculty of Medicine of Albacete, University of Castilla-La Mancha, Albacete, Spain | [2]Centre for Biomedical Research (CRIB), University of Castilla-La Mancha, Albacete, Spain | [3]ITEAM Research Institute, Universitat Politècnica de València, Valencia, Spain

**Correspondence:** Jesus Gonzalez-Rubio (jesus.gonzalez@uclm.es) | Concepcion Garcia-Pardo (cgpardo@iteam.upv.es)

**Received:** 20 December 2024 | **Revised:** 19 June 2025 | **Accepted:** 11 August 2025

**Funding:** This study was supported by the EMERGE-5G project Ref. PID2020-115005RJ-I00, Ramon & Cajal fellowship RYC2021-033207-I, HEROE-6G project Ref. CNS2023-143570 granted all by the Spanish Agency for Research MCIN/AEI/10.13039/501100011033, European Union NextGenerationEU/PRTR, the Program Investigo (INVEST/2022/199), held by the Conselleria de Innovación, Universidades, Investigación y Sociedad Digital de la Generalitat Valenciana, funded by Next Generation EU within the framework Plan de Recuperación, Transformación y Resiliencia de España.

**Keywords:** 5G networks | human exposure | kriging: EMF exposure, measurements, code-selective

## ABSTRACT

This study evaluates radiofrequency electromagnetic field (RF-EMF) exposure in 5G networks using a dual approach that combines theoretical extrapolations and direct measurements in diverse semiurban and urban environments, specifically on the campus of the Polytechnic University of Valencia. Measurements were conducted using personal exposimeters under active traffic conditions on the 5G network, complemented by a code-selective measurement system based on an R&S TSME6 scanner. This approach enabled the calculation of maximum theoretical exposure by detailed analysis of 5G signals and the capture of key parameters such as cell ID and beam indices at 16 representative points across the campus. For precise spatial visualization, Kriging interpolation techniques in ArcGIS were employed to generate continuous exposure maps illustrating the spatial distribution of RF-EMF in the study area. The results indicate that both the extrapolated theoretical values and measured levels align with the limits recommended by the ICNIRP, even under high data demand scenarios, supporting current safety assessments of 5G infrastructure regarding electromagnetic exposure. The correlation between theoretical and instantaneous exposures validates the applied methodology and its effectiveness in assessing exposure in diverse environments. This study provides a robust framework for future research and highlights the importance of continuous monitoring to ensure public safety during the deployment of new telecommunications infrastructure in urban areas. Bioelectromagnetics. 00:00–00, 2025. © 2025 Bioelectromagnetics Society.

## 1 | Introduction

Over the last decade, the global implementation of fifth-generation (5G) networks has revolutionized mobile connectivity by offering higher data speeds, lower latencies, and increased capacity for simultaneously connected devices (Andrews et al. 2014). This infrastructure is not only designed to enhance user experiences in everyday services but also to support the Internet of Things (IoT) and enable real-time applications requiring high reliability, such as telemedicine and industrial automation (Boodai et al. 2023). However, as with previous technologies, the deployment of 5G networks

Alberto Najera and Alvaro Villaescusa-Tebar contributed equally to this study.

**Summary**

- We conducted a dual evaluation of RF-EMF exposure in 5G through direct measurements and theoretical extrapolations.
- Spatial exposure maps were developed using Kriging interpolation for detailed visualization.
- We confirmed that exposure levels are significantly below ICNIRP safety limits.

has raised concerns about the potential health effects of exposure to radiofrequency electromagnetic fields (RF-EMF) (Chiaraviglio et al. 2022; Karipidis et al. 2021; Liu et al. 2024).

The debate on the safety of mobile technologies revolves around RF-EMF exposure. The International Commission on Nonionizing Radiation Protection (ICNIRP) has established safe exposure limits, asserting that exposure levels from 5G networks fall within these safety thresholds (International Commission on Nonionizing Radiation Protection [ICNIRP] 2020). Most studies support this conclusion, indicating that 5G technology does not pose significant adverse effects when exposure limits are respected (Bonato et al. 2022). Nevertheless, specific features of 5G networks, such as the use of higher frequencies and beamforming techniques, introduce new challenges in accurately assessing RF-EMF levels in real-world scenarios. According to Korkmaz et al. (2024), these characteristics make precise predictions of exposure in diverse environments difficult, prompting further research to optimize measurement methodologies and ensure accuracy in this evolving landscape.

Among classical methodologies for measuring personal exposure, mobile exposimeters allow for practical real-time RF-EMF exposure capture (Bolte et al. 2011; Frei et al. 2009). Another option includes low-cost sensors designed to withstand various environmental conditions and perform continuous measurements in both stationary and mobile evaluations. While useful for individual studies and distributed exposure networks across large areas, these devices still have limitations in terms of measurement precision and uncertainty for RF-EMF. Conversely, code-selective measurements enable a detailed assessment of different components of 5G signals, facilitating the identification of individual contributions from operators, cells, and beams (Keller 2019). These measurements are essential for calculating exposure under maximum theoretical load scenarios, providing a context for understanding exposure levels in extreme situations, which can be compared with instantaneous exposure measurements during peak forced load conditions.

Although various studies have explored different extrapolation methods, most focus on estimating theoretical maximum exposure without considering instantaneous RF-EMF exposure values in real conditions (Aerts et al. 2023; Deprez et al. 2022). Recently, a study addressed this limitation by comparing theoretical maximum exposure with instantaneous measurements under real traffic conditions, providing a practical reference for evaluating exposure in urban environments (Villaescusa-Tebar et al. 2024). Lastly, regarding the spatial representation of exposure levels, Gonzalez-Rubio et al. (2016) demonstrated how Geographic Information System (GIS) tools facilitate detailed mapping of RF-EMF distribution in urban and semiurban areas, even encompassing an entire city. This technique not only enables detailed exposure visualization but also makes data more accessible and understandable for quick interpretation, which is crucial for risk management and public communication.

In this context, new studies are required to investigate 5G network exposure under real conditions. Inspired by some of these techniques, our study combines theoretical extrapolation with direct measurements and a detailed spatial geostatistical analysis using GIS to provide a comprehensive view of RF-EMF exposure in 5G networks. This approach contributes to future research and enables the creation of clear and effective exposure maps, which are essential for evaluating public safety and understanding the impact of 5G technology on risk perception among the population. To our knowledge, this is the first study to integrate personal exposimeter measurements, code-selective 5G Standalone signal analysis, and spatial exposure modeling through Kriging interpolation within an operational SA network environment.

## 2 | Methods

This study was conducted on the campus of the Polytechnic University of Valencia, an extensive area of approximately 750,000 $m^2$ offering a rich variety of urban and semiurban environments. This diversity makes it an ideal location for analyzing RF-EMF exposure under realistic and controlled conditions. The selection of this campus was based not only on its representativeness in academic and demographic terms but also on its architectural design and spatial layout, which help minimize signal interference and enable precise exposure mapping. Furthermore, this environment facilitates a detailed spatial analysis using Geographic Information Systems (GIS), allowing the creation of exposure maps that enhance the interpretation of data (Figure 1).

To collect data, 16 measurement points were strategically distributed across the campus to capture the environmental heterogeneity in key locations such as open areas, academic buildings, and recreational zones. The placement of these measurement points followed an optimized design considering factors such as proximity to 5G antennas, pedestrian and vehicular traffic patterns, and fluctuations in occupancy density at different times of the day. Additionally, a preliminary environmental analysis was conducted to identify and mitigate potential sources of interference, such as high-power electronic equipment, industrial structures, and dense vegetation, which could affect signal propagation. This meticulous selection of points and conditions ensures that the results accurately reflect RF-EMF exposure conditions in a controlled urban environment.

### 2.1 | RF-EMF Measurement Methodology

To measure RF-EMF exposure, a dual methodology was implemented, combining the use of personal exposimeters with a

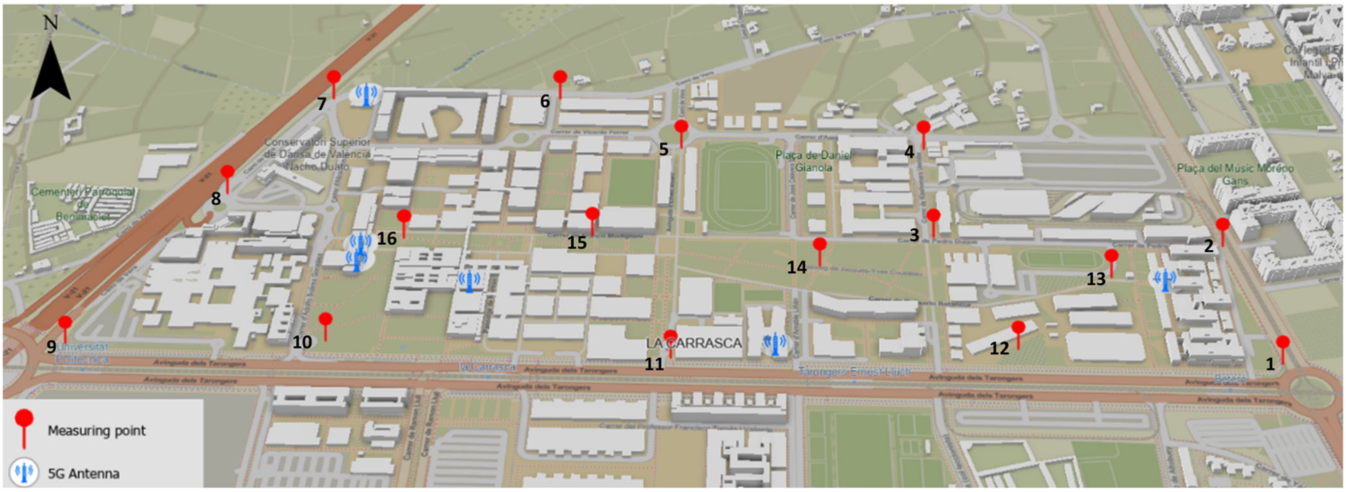


**FIGURE 1** | Measurement area. Polytechnic University of Valencia, Spain. Blue, antennas; Red, measurement points.

code-selective measurement system. This comprehensive approach allowed for the detailed capture of data on the intensity and specific profiles of RF-EMF signals present on the campus, originating from three distinct 5G network operators (A, B, and C). The presence of multiple operators in the study area added complexity and relevance to the analysis, enabling the evaluation of combined exposure from various sources.

For direct measurements, a high-sensitivity personal exposimeter (EME Spy Evolution) was used, capable of continuously recording variations in the RF-EMF spectrum at key 5G frequencies. These devices provided a reliable basis for assessing environmental exposure and the user's immediate surroundings. Additionally, the use of an R&S TSME6 scanner for code-selective measurements enhanced analytical precision by identifying signals exclusively emitted by 5G antennas. This component focuses solely on measuring the synchronization signal block (SSB), enabling not only the evaluation of overall exposure but also the specific characterization of exposure sources, helping to distinguish between operators, cells, and beams.

This methodology provided highly detailed data that, combined with GIS analyses, were used to construct a comprehensive spatial model of RF-EMF exposure across various zones of the campus (Figure 2).

A series of measurements was conducted at 16 strategically distributed points across the campus, focusing on capturing RF-EMF exposure under active 5G network traffic conditions. To replicate a real-use scenario, a User Equipment (UE) device was exclusively configured to the 5G network, operating continuously during each session to generate and receive data, simulating intensive traffic conditions.

Each measurement session lasted 6 min, with data recorded at 10-second intervals, enabling the capture of signal intensity and other relevant parameters. This sampling interval allowed for a dynamic evaluation of exposure, observing variability in RF-EMF levels under active 5G traffic conditions. The exposimeters continuously recorded RF-EMF levels, while the code-selective measurement equipment precisely identified 5G synchronization signals, differentiating between signal types within the spectrum.

To ensure consistency and precision, all equipment underwent calibration and synchronization before each session. This approach not only facilitated the measurement of general exposure but also enabled the analysis of specific network components and their contributions to overall exposure.

## 2.2 | Uncertainty Budget and Data Adjustment

An uncertainty analysis was conducted to assess the reliability of the exposure measurements obtained with both the personal exposimeter (EME Spy Evolution) and the code-selective method using the R&S TSME6 scanner. For the exposimeter, the main sources of uncertainty considered include calibration uncertainty specified by the manufacturer (±1.5 dB, typically translating to ~20% in real-world scenarios), environmental variability due to reflections, obstacles, and user movement, as well as limitations in antenna directivity and device positioning. These factors are well-documented in previous studies (Bolte 2016; Frei et al. 2009) and contribute to a combined uncertainty that, according to practical assessments, is commonly considered in the range of ±20%–25% for personal RF-EMF exposure measurements under field conditions (IEC 62232:2022). This estimate accounts for both systematic and random errors inherent to real-life measurement campaigns.

Regarding code-selective measurements, the uncertainty of the levels provided can come from different sources: (1) the uncertainty of the R&S TSME6 scanner, which the manufacturer reported to be below 1.5 dB (©Rohde & Schwarz; R&S TSME6 Ultracompact Drive Test Scanner) for the studied frequencies leading to ±41% of the SSB power levels maximum; (2) the load of the user that according to several studies can range up to around 30 dB in worst cases in the extrapolated electric field strength; and (3) some other sources such as the antenna, the environment, and the equipment calibration. Some studies with a similar setup quantifies this source as 2.39 dB (Expósito et al. 2024). All uncertainties reported in dB refer to

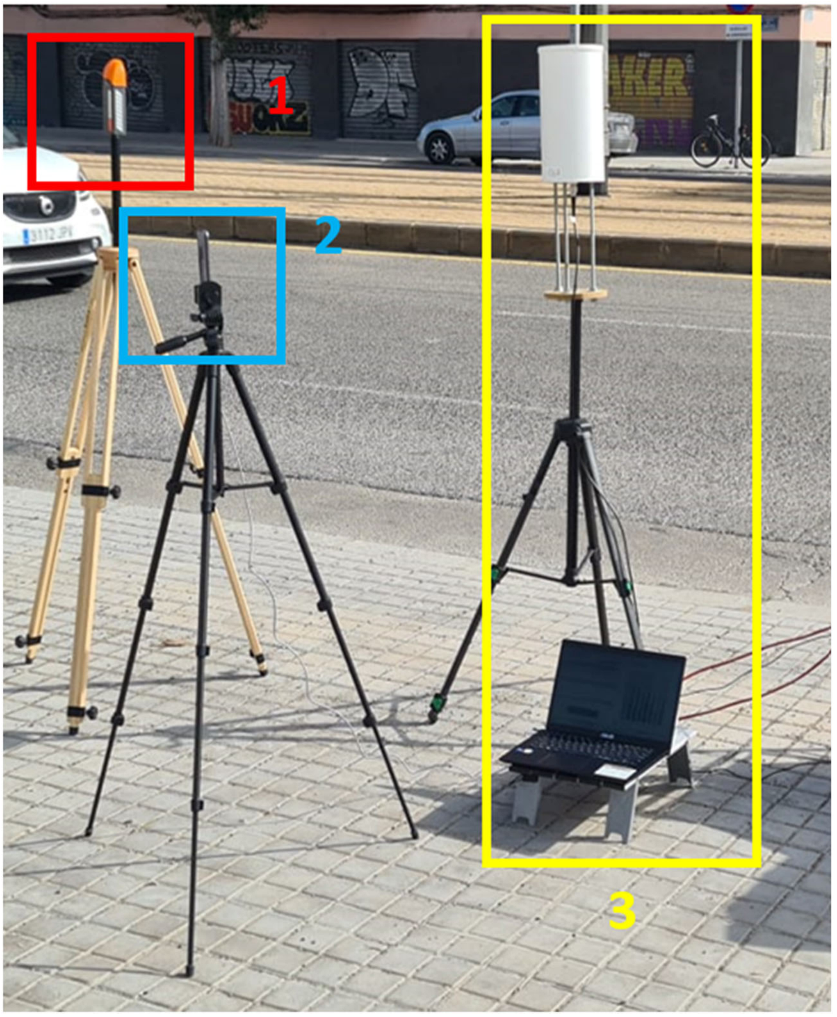


**FIGURE 2** | Measurement setup: 1. Personal exposimeter; 2. User equipment (UE) for generating 5G traffic; 3. Code-selective measurement equipment.

electric field strength (E-field) measurements. Percentage values refer to manufacturer-specified tolerances associated with the RSS readings of the 5G synchronization signal block (SSB) obtained by the R&S TSME6 scanner. These percentage uncertainties apply to the direct signal strength measurements, not to the final exposure estimates derived from them.

## 2.3 | Theoretical Maximum Exposure Calculation Procedure

In the studied environment, signals from three 5G network operators (A, B, and C) were identified. For this study, RF-EMF exposure data were obtained and processed separately for each network operator. However, only the values corresponding to operator B were extrapolated to the theoretical maximum, as it was the only operator generating active traffic during the measurement period. This approach allows for an estimation of the theoretical maximum exposure scenario under realistic network usage conditions.

From the scanner-provided data, specific parameters were selected, including the physical cell ID (PCI), beam indices, and reference signal received power (RSRP) from the synchronization signal block (SSB). These parameters are essential for understanding the distribution of 5G signals at each measurement point across the campus.

For the measurements, an omnidirectional Cobham OA2-0.3-10.0 V/1505 antenna (0.4–10 GHz) was used, with its detailed radiation patterns available for analysis.

## 2.4 | Theoretical Maximum Exposure Calculation

The theoretical maximum exposure can be deduced from the power of the synchronization signal (SSS) of one of the beams, as follows (Aerts et al. 2023; Keller 2019):

$$E_{\mathrm{PCI}}^{\max} = E_{\mathrm{RE}}^{SSB} \cdot N_{\mathrm{SC}} \cdot \sqrt{F_{\mathrm{TDC}} \cdot K_{\mathrm{antenna}} \cdot K_{\mathrm{stat}}} \tag{1}$$

where $E_{\mathrm{RE}}^{\mathrm{SSB}}$ is the electric field in V/m of the SSS for all the beams in the cell, $N_{\mathrm{SC}}$ is the total number of subcarriers in the 5G channel, $F_{\mathrm{TDC}}$ represents the TDD duty cycle, $K_{\mathrm{antenna}}$ is a correction factor dependent on the gain ratio between traffic and synchronization beams, and $K_{\mathrm{stat}}$ denotes the ratio between the radiated power for synchronization and traffic signals.

It is worth noting that $F_{\mathrm{TDC}}$, $K_{\mathrm{antenna}}$, and $K_{\mathrm{stat}}$ are parameters that can be estimated. However, for more accurate values, these parameters should ideally be provided by the respective telecommunications operators. A simplified version of this equation, assuming a worst-case scenario, is as follows:

$$E_{\mathrm{PCI}}^{\max} = E_{\mathrm{RE}}^{\mathrm{SSS}} \cdot N_{\mathrm{SC}} \tag{2}$$

where $N_{\mathrm{SC}}$ is calculated as:

$$N_{\mathrm{SC}} = \sqrt{\frac{\mathrm{BW}}{\mathrm{SCS}}} \tag{3}$$

Here, BW represents the channel bandwidth, and SCS is the subcarrier spacing of the signal. To derive the incident electric field per Resource Element (RE) from SSS_RSRP, the following conversion using the antenna factor or effective antenna area is applied:

$$E_{\mathrm{RE}}^{\mathrm{SSS}} = \sqrt{\frac{\mathrm{SSS\_RSRP}}{A_{ef}} \cdot \eta_0} \tag{4}$$

where $\eta_0$ is the intrinsic impedance of free space, and $120\pi$ ($\Omega$) and $A_{ef}$ is the effective area of the antenna, which can be calculated from the antenna gain. For precise gain computation, an interpolation at the exact channel frequency is performed using the data provided by the antenna manufacturer.

The R&S TSME6 scanner instrument measures power values for each beam at individual time points. To ensure consistency, electric field values are averaged in 1-second bins, producing a singular value for each beam associated with a PCI over the 6-min measurement period.

The electric field for a PCI is then calculated by summing the contributions of all beams:

$$E_{\mathrm{PCI}}^{\mathrm{sss}} = \sqrt{\sum_{\mathrm{beams}} \left(E_{\mathrm{PCI,beam}}^{\mathrm{SSS(RE)}}\right)^2} \tag{5}$$

By substituting $E_{\mathrm{PCI}}^{\mathrm{sss}}$ into Equation (2), the theoretical maximum exposure for a PCI is computed.

Finally, a theoretical maximum exposure value per operator at each measurement point is obtained:

$$E_{\mathrm{operator}}^{\max} = \sqrt{E_{\mathrm{PCI}_1}^{2\max} + E_{\mathrm{PCI}_2}^{2\max} + E_{\mathrm{PCI}_n}^{2\max}} \tag{6}$$

Using $E_{\mathrm{operator}}^{\max}$, values from different operators can be summed to calculate a single exposure value per point.

## 2.5 | Instantaneous Exposure Calculation Procedure

The instantaneous exposure was assessed using data collected by the EME Spy Evolution personal exposimeter, which continuously recorded RF-EMF levels at key 5G frequencies during each 6-min measurement session. Measurements were taken every 10 s, resulting in 36 individual readings per session. To ensure data consistency, values below the device's detection threshold were discarded.

The raw data were then processed to calculate average and median values for each measurement point, providing a robust representation of the exposure levels in real-world conditions. Statistical analyses, including Spearman and Pearson correlation tests, were performed to compare the exposimeter results with theoretical maximum exposure values. These analyses validated the consistency and reliability of the instantaneous exposure data.

To mitigate potential biases, all measurements were conducted under controlled conditions, and calibration procedures were performed before each session. This approach ensured the accuracy of the exposimeter readings and their applicability for evaluating environmental RF-EMF exposure in diverse 5G scenarios.

## 2.6 | Downlink Traffic Simulation Procedure in the 5G Network

To evaluate exposure under high-demand conditions, we configured an intensive traffic scenario using a 5G-compatible mobile device. This device was specifically chosen for its ability to handle high data transfer rates over 5G, ensuring that all transmissions occurred exclusively on the 5G network without switching to older network technologies such as 4G or WiFi.

We simulated intensive data usage by downloading and streaming high-quality videos (2160p), replicating typical high-demand daily usage scenarios. During these simulations, traffic was closely monitored to confirm that the device remained within the 5G band. Advanced configuration tools such as Android Debug Bridge (ADB) were employed to lock the network mode to 5G, ensuring that the collected data reflected exposure exclusively attributable to this technology.

## 2.7 | Data Analysis

To process the collected data, we performed a comprehensive analysis using R and SPSS. A central element of this analysis was the comparison between theoretical exposure levels and real-world measurements, which included a detailed examination of exposure variability across different points on the campus. The data were centralized on an analysis platform to evaluate variability and correlations between measurements.

Normality tests (Kolmogorov–Smirnov) were conducted to assess the distribution of the data. The results ($p$-value $< 0.05$) indicated that the data did not follow a normal distribution. Consequently, Spearman's correlation was selected as the primary method to assess the association between exposimeter and scanner measurements. Pearson correlation coefficients were also reported to provide complementary information about linear association strength. These correlations offered a more complete perspective on the consistency and reliability of both measurement methods across varied network conditions.

### 2.8 | Visualization and Spatial Representation of Exposure Using Kriging

The Kriging interpolation technique was applied in ArcGIS Pro to visually represent the spatial distribution of RF-EMF exposure across the campus, creating a continuous exposure map based on specific measurement points. This process not only estimated exposure levels in unsampled areas but also provided a measure of uncertainty, adding reliability and depth to the analysis. Although our Kriging interpolation was performed on a dense data set of RSS measurements from the TSME6 scanner, this geostatistical method inherently introduces interpolation uncertainty. Previous RF-EMF mapping studies in comparable outdoor environments have shown average relative errors of approximately ±2 dB when using well-distributed measurement points (Aerts et al. 2013).

The generated map, based on a carefully adjusted semivariogram reflecting spatial variability, offers an intuitive interpretation of how exposure changes throughout the campus. This visualization is critical for identifying patterns and areas of higher or lower exposure in a clear and comprehensible manner, facilitating the interpretation of data beyond individual measurement figures.

The spatial representation in the map serves as a powerful tool for communicating complex findings, enabling both the academic community and policymakers to easily understand the distribution of exposure and make informed decisions. For this study, ordinary Kriging was used as the interpolation method, as it provides a reliable estimation of spatial variability based on measured points without assuming a global trend. A spherical semivariogram model was selected after exploratory analysis of the empirical semivariogram, as it best represented the spatial correlation of the measured RF-EMF levels. Model parameters were optimized to minimize the root mean square error (RMSE) during cross-validation, ensuring an accurate interpolation of exposure levels across the campus. Furthermore, this approach provides a robust foundation for future research and safety evaluations of 5G network infrastructure, maximizing the utility of the collected data.

## 3 | Results

The exposure measurements obtained at the 16 points distributed across the campus revealed that both the theoretical maximum exposure values and the field measurements were significantly below the ICNIRP-established safety limits ($10\ W/m^2$).

Table 1 presents the exposure measurements at each of the 16 sampling points on the campus. The Total Received Signal Strength (RSS), obtained through code-selective measurements of the Synchronization Signal Block (SSB) and representing the

**TABLE 1** | Power density under traffic conditions: Comparison between theoretical maximum exposure and instantaneous exposure recorded at campus sampling points.

| ID | X | Y | RSS Total ($mW/m^2$) | Exposimeter (mean $mW/m^2$) | Exposimeter (median $mW/m^2$) |
|---|---|---|---|---|---|
| 1 | 729353.60 | 4373088.31 | 416.16 | 6.90 | 39.89 |
| 2 | 729384.58 | 4373294.90 | 1814.85 | 13.37 | 20.01 |
| 3 | 729021.60 | 4373427.73 | 378.18 | 3.83 | 7.92 |
| 4 | 729076.71 | 4373594.61 | 1353.83 | 15.73 | 27.19 |
| 5 | 728748.59 | 4373700.01 | 45.48 | 2.72 | 4.10 |
| 6 | 728610.84 | 4373855.74 | 33.55 | 3.44 | 4.70 |
| 7 | 728295.68 | 4373954.83 | 626.55 | 55.00 | 59.12 |
| 8 | 728123.80 | 4373798.03 | 1269.19 | 11.91 | 20.50 |
| 9 | 727895.17 | 4373579.65 | 702.76 | 7.04 | 13.66 |
| 10 | 728211.81 | 4373485.7 | 540.10 | 5.49 | 10.76 |
| 11 | 728622.21 | 4373327.43 | 22.16 | 20.08 | 22.90 |
| 12 | 729046.56 | 4373210.01 | 86.21 | 3.17 | 7.09 |
| 13 | 729216.63 | 4373288.47 | 4359.85 | 343.77 | 383.80 |
| 14 | 728857.10 | 4373422.39 | 71.53 | 4.46 | 8.52 |
| 15 | 728582.95 | 4373568.07 | 142.43 | 3.76 | 3.97 |
| 16 | 728340.89 | 4373638.43 | 69.68 | 2.89 | 2.82 |

*Note:* Exposimeter values are subject to an estimated overall uncertainty of ±25%, accounting for calibration, body influence, environmental variability, and device characteristics (Bolte 2016; Frei et al. 2009; IEC 62232:2022). Theoretical maximum values (RSS Total), derived from code-selective measurements with the R&S TSME6 scanner, are associated with an estimated uncertainty of ±20%, considering scanner calibration, extrapolation models, and signal variability (Expósito et al. 2024; Keller 2019). These uncertainties are inherent to real-life RF-EMF measurement campaigns and have been considered in the analysis.

extrapolated theoretical maximum power density, varies considerably, with a maximum of 4359.85 mW/m² recorded at point 13 and a minimum of 22.16 mW/m² at point 11. This wide variability in exposure levels can be attributed to factors such as proximity to antennas and the physical characteristics of the environment (e.g., buildings or open areas). The exposimeter measurements, including both mean and median values, generally reflect low levels compared to the ICNIRP exposure limits. The mean values recorded by the exposimeter range from 2.72 mW/m² (point 5) to 343.77 mW/m² (point 13), while the median values range from 2.82 to 383.80 mW/m². It is important to note that the exposimeter readings represent the total RF-EMF exposure detected at each measurement point, which may include contributions from other background signals or interference not captured in the RSS total values calculated from synchronization signals. These differences are expected due to the broader sensitivity of the exposimeter, which accounts for all sources within its detection range, whereas the RSS total specifically measures contributions from the 5G synchronization signals. Notably, point 13 showed the highest exposure levels in both RSS and exposimeter readings, consistent with its location and fewer obstructions.

Even at the points of highest exposure, the recorded RF-EMF levels remain significantly below the ICNIRP safety limit of 10 W/m². These findings confirm the safety of the 5G infrastructure on campus in terms of electromagnetic exposure, suggesting that exposure levels in this environment are within a safe range and do not pose a health risk.

This detailed analysis of the data in Table 1 supports the reliability of the measurements and provides a solid foundation for future research and safety evaluations in the deployment of 5G networks in similar environments.

### 3.1 | Correlation Analysis Between RSS and Exposimeter Measurements

To quantify the relationship between RSS measurements and the values obtained using the exposimeter, Pearson and Spearman correlation analyses were performed. The results show significant correlation coefficients, indicating a strong association between the two metrics.

The Pearson correlation coefficients for the median and mean of the exposimeter measurements were 0.8886 and 0.8807, respectively, with $p$-values $< 0.001$, suggesting a significant linear relationship. Similarly, the Spearman correlation coefficients were also significant (0.6294 for the median, $p$-value $= 0.01$, and 0.6471 for the mean, $p$-value $= 0.01$), further supporting the consistency of the exposure measurements.

These findings indicate that the exposimeter values accurately reflect environmental exposure and align with the RSS data, validating the reliability and precision of the measurement methods used in this study.

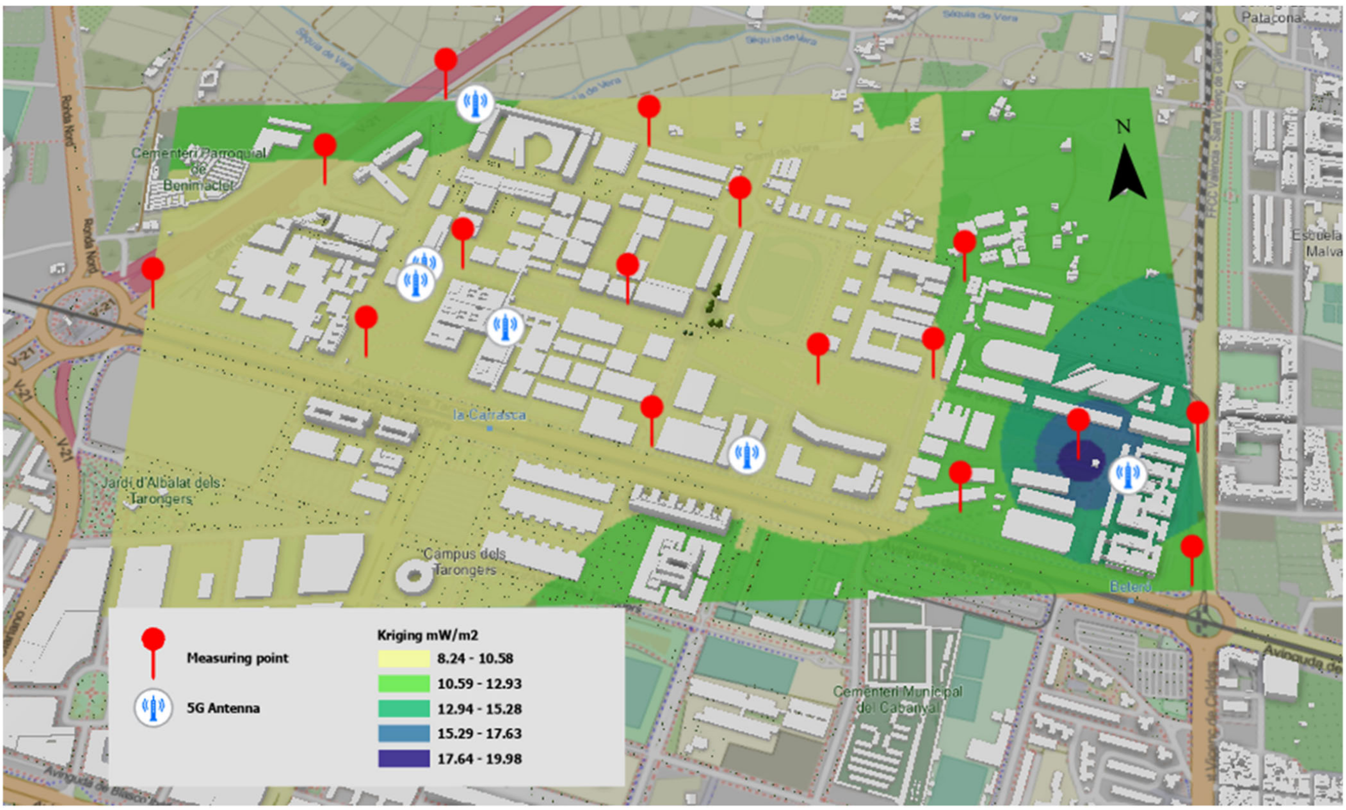


**FIGURE 3** | Spatial distribution of RF-EMF exposure levels based on instantaneous measurements obtained with the personal exposimeter (EME Spy Evolution). Values represent the mean electric field recorded at each measurement point, interpolated using Ordinary Kriging. This map reflects real-world exposure under active 5G network traffic conditions.

### 3.2 | 5G Radiation Maps Using Kriging Interpolation

Kriging maps provide a detailed visual representation of the spatial distribution of RF-EMF exposure on the campus, distinguishing between instantaneous exposure measurements and theoretical maximum exposure estimates.

Figure 3 depicts the radiation levels based on instantaneous measurements captured by the exposimeter under real traffic conditions. The map features a color gradient ranging from green to blue, where green areas represent zones of lower exposure, and blue areas indicate relatively higher exposure. This gradient facilitates the visual identification of high- and low-exposure zones, illustrating how RF-EMF levels vary with proximity to emission sources.

Figure 4 illustrates the calculated theoretical maximum exposure, extrapolated for a scenario of maximum traffic density. This map also uses a similar color gradient to highlight power density intensity across the campus. Comparing the two maps reveals that while instantaneous measurements indicate relatively low exposure in most areas, theoretical estimates show higher peaks near antennas, providing insights into network behavior under maximum load scenarios.

Measurement points, marked with red dots, indicate the specific locations where exposure data were collected, forming the basis for the Kriging interpolation model. These points are critical for ensuring interpolation accuracy, as they enable the estimation of values in unsampled areas based on real data. Additionally, blue icons indicate the locations of RF-EMF emission sources (antennas), whose proximity to the measurement points directly impacts local exposure levels.

The spatial interpolation obtained through Kriging offers an intuitive and precise understanding of how the 5G network infrastructure distributes exposure levels across the campus. This approach helps identify areas that may require additional considerations to minimize exposure. Such visual representation is an effective tool for clearly and comprehensively communicating findings to both the scientific community and policymakers, providing a robust foundation for future evaluations and decisions in 5G infrastructure management.

## 4 | Discussion

This study evaluated RF-EMF exposure levels in a 5G network environment using a dual approach comprising direct measurements and theoretical estimates. By conducting measurements on a university campus with controlled and simulated network traffic, we gained deeper insights into how network traffic and infrastructure configurations influence exposure levels in everyday scenarios. The results, which remained significantly below the ICNIRP safety limits, align with

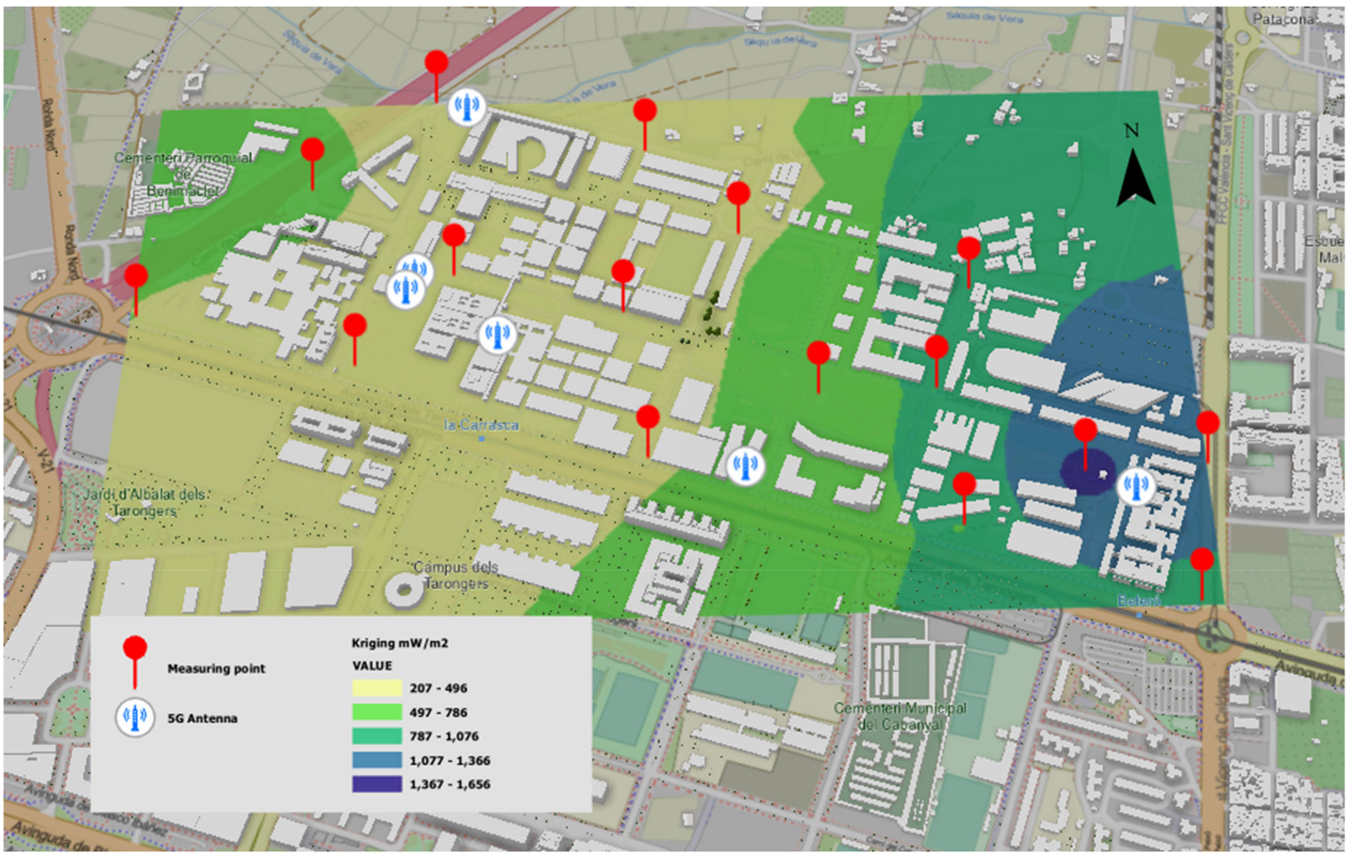


**FIGURE 4** | Spatial distribution of RF-EMF exposure based on theoretical maximum values estimated from synchronization signal (SSB) power readings recorded by the R&S TSME6 code-selective scanner. Kriging interpolation was applied to the maximum extrapolated electric field values at each point, simulating worst-case 5G exposure scenarios under full network load.

accumulated evidence from other studies on the safety of 5G technology in urban and semiurban settings.

Compared to previous research, our findings are consistent with recent studies indicating safe exposure levels in 5G networks. For instance, Karipidis et al. (2021) reported that 5G base stations in urban areas generate exposure levels within safe limits, supporting our observations in the academic context studied. Similarly, Bonato et al. (2022) observed comparable levels in high-traffic environments across Europe, validating our findings and confirming the safety of RF-EMF exposure under controlled traffic and elevated data usage conditions. Moreover, Aerts et al. (2023) demonstrated that exposures in small cell 5G environments remain low, confirming that modern infrastructure can minimize RF-EMF exposure even under high traffic conditions. Additionally, Wali et al. (2022) showed that increased traffic marginally raises exposure levels, consistent with our observations that the use of an active device on campus only moderately increases exposure without reaching critical thresholds.

Our study also highlights the relevance of the spatial representation of exposure data. Using GIS tools, such as Kriging spatial analysis, allowed us to visualize the variable distribution of 5G signals across different campus zones. This approach complements studies like Gonzalez-Rubio et al. (2016), who also utilized GIS to map exposure across an entire city, providing a practical perspective on exposure in large urban and semiurban areas. At the same time, it is important to consider that spatial interpolation methods, including Ordinary Kriging, inherently involve a degree of uncertainty. Estimations in areas distant from measurement points may be less precise, and results should therefore be interpreted with appropriate caution, especially in heterogeneous environments.

By integrating spatial analysis into our study, we improved accessibility and comprehension of exposure data, offering clear and detailed visual tools for the academic community and policymakers to evaluate exposure distribution and associated risks in a university setting. By systematically comparing theoretical extrapolations with real-world measurements in an active 5G environment, our study provides a replicable framework that strengthens exposure assessment methodologies and supports evidence-based decisions for future network deployments. The integration of Geographic Information Systems further enhances the practical application of these results, enabling more effective spatial analysis and visualization for exposure management and public communication.

### 4.1 | Limitations

Despite the robustness of our methodology, this study has some limitations. One major limitation is the reliance on extrapolation factors provided by telecommunications operators, which were not always precise or fully available. This limitation may affect the accuracy of our theoretical exposure estimates. Collaborating with operators to obtain detailed data on traffic patterns and specific base station configurations would be essential to refine predictive models and optimize future measurements (Wali et al. 2022).

Additionally, the physical infrastructure of the campus, with its variety of buildings and structures, may have influenced RF-EMF measurements. Variability in architectural conditions suggests the need for additional studies in more homogeneous or diverse environments to better understand how environmental characteristics affect exposure.

Future research should expand the scope of this study to other environments, such as indoor settings or areas with higher population density, to gain a more comprehensive view of exposure across various usage scenarios. Collaboration with telecommunications operators could further refine base station configurations and extrapolation models, enhancing the accuracy and applicability of results in diverse contexts (Aerts et al. 2023).

Moreover, this study highlights the potential for further development in spatial representation techniques, such as 3D Kriging or similar interpolation methods, to generate exposure maps that account for the vertical dimension of measurements. Implementing advanced measurement technologies, coupled with closer collaboration with network operators, will facilitate ongoing and precise RF-EMF exposure evaluation.

Furthermore, we have now clarified the specific Kriging interpolation method used (Ordinary Kriging) and included a discussion on its associated uncertainties. In particular, we provide details on the semivariogram model applied (spherical), its goodness of fit, and the cross-validation results, which support the reliability of the spatial interpolation. Nonetheless, it is important to acknowledge that interpolation methods inherently carry uncertainty, especially in areas farther from measurement points, and their results should be interpreted accordingly. While independent validation measurements were not conducted in this study, we acknowledge this as a limitation. Future studies should consider external control measurements or cross-validation techniques to further strengthen the spatial exposure model.

Additionally, the physical infrastructure of the campus, with its variety of buildings and structures, may have influenced RF-EMF measurements. Variability in architectural conditions suggests the need for additional studies in more homogeneous or diverse environments to better understand how environmental characteristics affect exposure (Figure 4).

Although the technical uncertainties of both devices range between 2 and 3 dB, differences greater than 10 dB were observed at certain points. These discrepancies can be explained by differences in measurement dynamics: the exposimeter records averaged values over time, whereas the TSME6 captures instantaneous values with high spectral and spatial resolution. Additional variability may arise from environmental obstructions or fluctuating network traffic during acquisition, which can differentially affect each device even under tripod-mounted, static measurement conditions (Bolte and Eikelboom 2012; Sagar et al. 2018).

Finally, education and communication about the risks and benefits of 5G technology are crucial to ensure public acceptance and promote informed and safe integration into daily life. This study provides robust evidence supporting the safety of 5G networks regarding RF-EMF exposure, confirming that exposure levels remain well below ICNIRP-recommended limits. It also underscores the importance of implementing accurate and controlled measurement methodologies to assess exposure in real-world environments.

### Conflicts of Interest

The authors declare no conflicts of interest.

### References


Aerts, S., K. Deprez, L. Verloock, et al. 2023. "RF-EMF Exposure Near 5G NR Small Cells." *Sensors* 23: 3145.

Aerts, S., D. Deschrijver, L. Verloock, T. Dhaene, L. Martens, and W. Joseph. 2013. "Assessment of Outdoor Radiofrequency Electromagnetic Field Exposure Through Hotspot Localization Using Kriging-Based Sequential Sampling." *Environmental Research* 126: 184–191.

Andrews, J. G., S. Buzzi, W. Choi, et al. 2014. "What Will 5G Be?" *IEEE Journal on Selected Areas in Communications* 32: 1065–1082.

Bolte, J. F. B. 2016. "Lessons Learnt on Biases and Uncertainties in Personal Exposure Measurement Surveys of Radiofrequency Electromagnetic Fields With Exposimeters." *Environment International* 94: 724–735.

Bolte, J. F. B., and T. Eikelboom. 2012. "Personal Radiofrequency Electromagnetic Field Measurements in the Netherlands: Exposure Level and Variability for Everyday Activities, Times of Day and Types of Area." *Environment International* 48: 133–142.

Bolte, J. F. B., G. van der Zande, and J. Kamer. 2011. "Calibration and Uncertainties in Personal Exposure Measurements of Radiofrequency Electromagnetic Fields." *Bioelectromagnetics* 32: 652–663.

Bonato, M., L. Dossi, S. Gallucci, M. Benini, G. Tognola, and M. Parazzini. 2022. "Assessment of Human Exposure Levels Due to Mobile Phone Antennas in 5G Networks." *International Journal of Environmental Research and Public Health* 19: 1546.

Boodai, J., A. Alqahtani, and M. Frikha. 2023. "Review of Physical Layer Security in 5G Wireless Networks." *Applied Sciences* 13: 7277.

Chiaraviglio, L., C. Lodovisi, D. Franci, et al. 2022. "EMF Exposure in 5G Standalone mm-Wave Deployments: What Is the Impact of Downlink Traffic?" *IEEE Open Journal of the Communications Society* 3: 1445–1465.

Deprez, K., L. Verloock, L. Colussi, et al. 2022. "In-Situ 5G NR Base Station Exposure of the General Public: Comparison of Assessment Methods." *Radiation Protection Dosimetry* 198: 358–369.

Expósito, I., C. Hakizimali, M. García Sánchez, I. Cuiñas, and J. Verhaevert. 2024. "Human Exposure to EMF From 5G Base Stations: Analysis, Evaluation and Comparison of Different Assessment Methods." *Measurement* 229: 114434.

Frei, P., E. Mohler, G. Neubauer, et al. 2009. "Temporal and Spatial Variability of Personal Exposure to Radio Frequency Electromagnetic Fields." *Environmental Research* 109: 779–785.

Gonzalez-Rubio, J., A. Najera, and E. Arribas. 2016. "Comprehensive Personal RF-EMF Exposure Map and Its Potential Use in Epidemiological Studies." *Environmental Research* 149: 105–112.

International Commission on Non-Ionizing Radiation Protection (ICNIRP). 2020. "Guidelines for Limiting Exposure to Electromagnetic Fields (100 kHz to 300 GHz)." *Health Physics* 118: 483–524.

Karipidis, K., R. Mate, D. Urban, R. Tinker, and A. Wood. 2021. "5G Mobile Networks and Health—A State-of-the-Science Review of the Research Into Low-Level RF Fields Above 6 GHz." *Journal of Exposure Science & Environmental Epidemiology* 31: 585–605.

Keller, H. 2019. "On the Assessment of Human Exposure to Electromagnetic Fields Transmitted by 5G NR Base Stations." *Health Physics* 117: 541–545.

Korkmaz, E., S. Aerts, R. Coesoij, et al. 2024. "A Comprehensive Review of 5G NR RF-EMF Exposure Assessment Technologies: Fundamentals, Advancements, Challenges, Niches, and Implications." *Environmental Research* 260: 119524.

Liu, S., K. Tobita, T. Onishi, M. Taki, and S. Watanabe. 2024. "Electromagnetic Field Exposure Monitoring of Commercial 28-GHz Band 5G Base Stations in Tokyo, Japan." *Bioelectromagnetics* 45: 281–292.

Sagar, S., S. Dongus, A. Schoeni, et al. 2018. "Radiofrequency Electromagnetic Field Exposure in Everyday Microenvironments in Europe: A Systematic Literature Review." *Journal of Exposure Science & Environmental Epidemiology* 28: 147–160.

Villaescusa-Tebar, A., A. Najera, J. Gonzalez-Rubio, and C. Garcia-Pardo. 2024. "Instantaneous Vs Theoretical Maximum Exposure Under Real Traffic Conditions: Example in the City of Valencia." In 2024, the 18th European Conference on Antennas and Propagation EUCAP. New York: IEEE. https://www.webofscience.com/wos/alldb/full-record/WOS:001215536200041.

Wali, S. Q., A. Sali, J. K. Allami, and A. F. Osman. 2022. "RF-EMF Exposure Measurement for 5G Over mm-Wave Base Station With MIMO Antenna." *IEEE Access* 10: 9048–9058.